

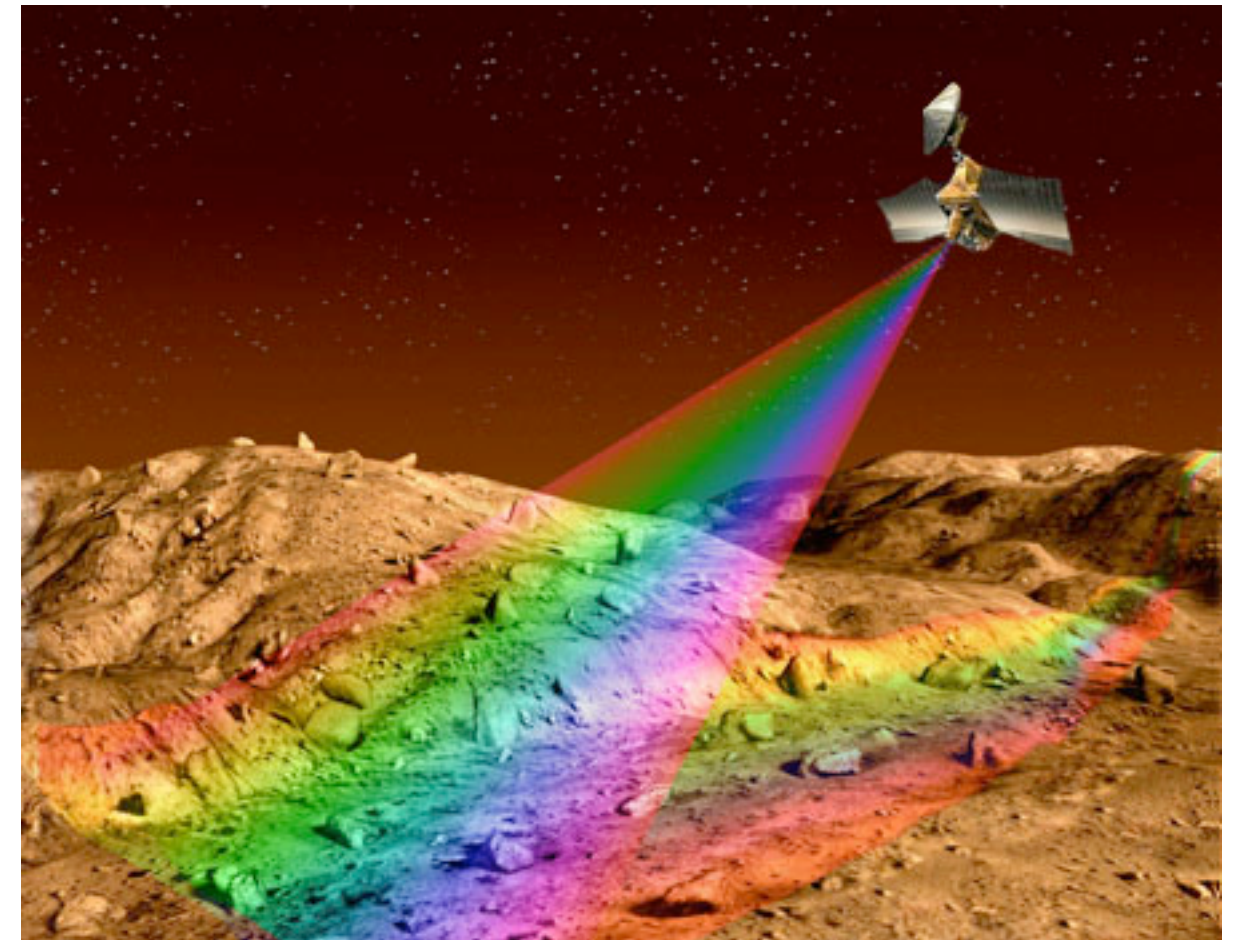
Mineralogical analysis using linear unmixing with group exclusivity constraints

Frédéric Schmidt^{1,2}, Sébastien Bourguignon³, Joanna Gurgurewicz⁴, Gaspard Salomon^{1,4}, Daniel Mège⁴

¹Université Paris-Saclay, CNRS, GEOPS, 91405, Orsay, France, ²Institut Universitaire de France ³LS2N, Ecole Centrale de Nantes, CNRS, 1 rue de la Noë, Nantes 44321, France ⁴Centrum Badań Kosmicznych Polskiej Akademii Nauk, Warsaw, Poland

Goal

- (semi-)supervised automatic detection for near-IR spectroscopy
- Summary (quick look) of the dataset
- Based on advance signal treatment and machine learning
- **NO PRECISE QUANTIFICATION**



Theory

- Estimation of **endmember spectra (lab)** and **abundances** under constraints:

Observation

Number of endmember

$$\mathbf{Y} = \sum_{i=1}^N \mathbf{A}_i \cdot \mathbf{S}_i$$

subject to
positivity
sum-to-one

A. Non-linearities ? grain size ? aerosols ?

B. Large endmember set ?

Theory

- Estimation of **endmember spectra (lab)** and **abundances** under constraints:

Observation

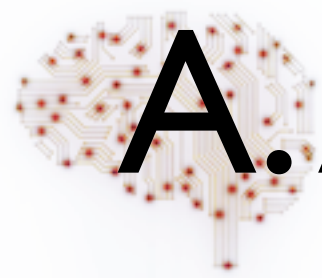
Number of endmember

$$\mathbf{Y} = \sum_{i=1}^N \mathbf{A}_i \cdot \mathbf{S}_i$$

subject to
positivity
sum-to-one

A. Non-linearities ? grain size ? aerosols ?

B. Large endmember set ?



A. Approximation of non-linearities

- Simple **non-linearity** of abundances, under constraints

Schmidt, F. Approximation of Radiative Transfer for Surface Spectral Features *IEEE Geoscience and Remote Sensing Letters*, Institute of Electrical and Electronics Engineers (IEEE), 2023, 20, 1-3, <http://dx.doi.org/10.1109/lgrs.2023.3263356>

$$\mathbf{Y} = \sum_{i=1}^N A_i \cdot \mathbf{S}_i^{\alpha} + \beta$$

- **Test of radiative transfer ?**
Shkuratov et al., 1999

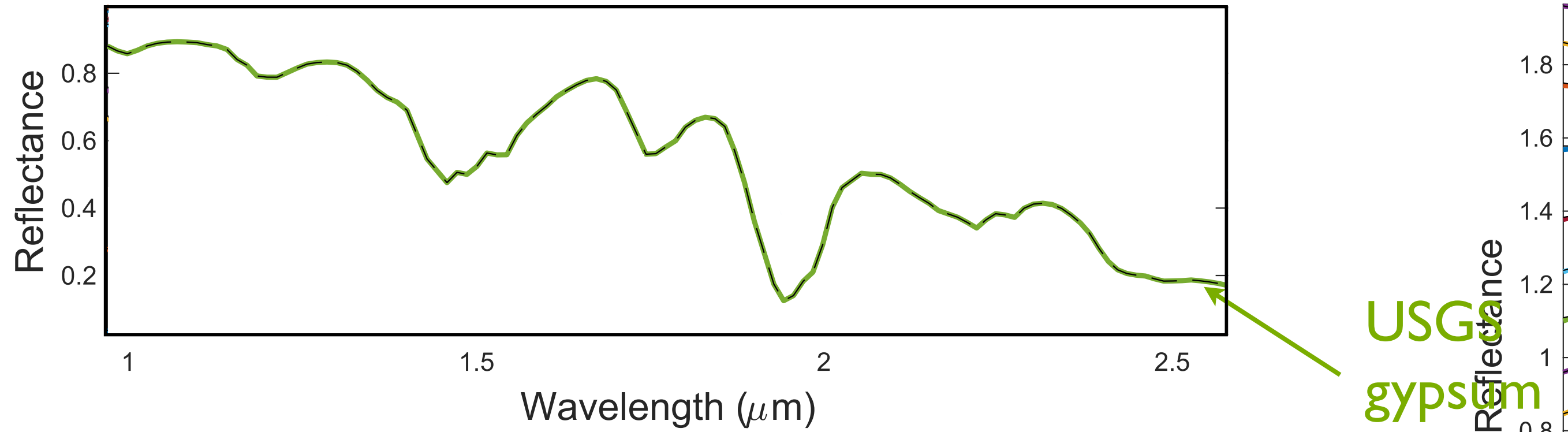
$$I = I_0 \cdot T(\theta_{em}) \cdot T(\theta_{in}) \cdot \exp\left(-\frac{\cos\theta}{\lambda} \sum_{v=0}^m S_v \sin\theta\right) \cdot \prod_{v=0}^m R(\theta_v), \quad (12)$$

$$r_b = R_b + \frac{T_e T_i R_i \exp(-2\tau)}{2 \int_0^{\pi/4} d\psi \int_0^{\pi/2} d\theta \cdot R_o(n, \theta) \cdot \cos\theta \cdot \sin\theta}, \quad (9a)$$

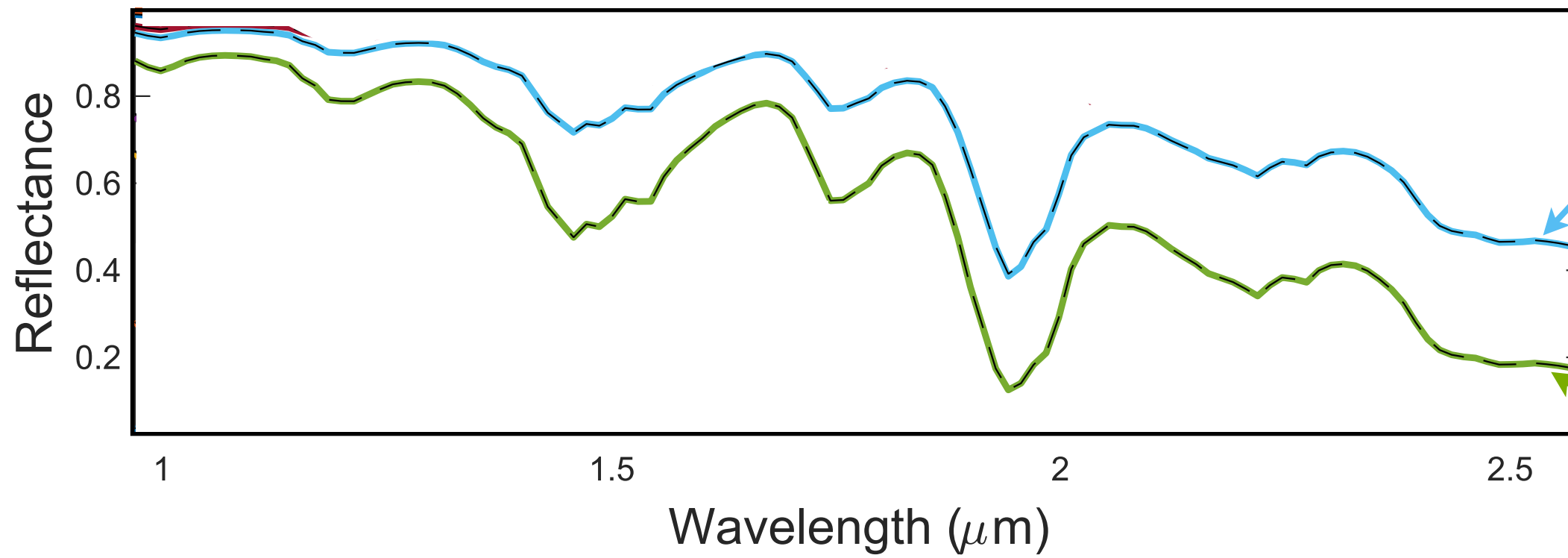
$$r_f = R_f + \frac{T_e T_i \exp(-\tau) + T_e T_o R_i \exp(-2\tau)}{2 \int_0^{\pi/4} d\psi \int_0^{\pi/2} d\theta \cdot R_o(n, \theta) \cdot \cos\theta \cdot \sin\theta}, \quad (9b)$$

$$A = \frac{1 + \rho_b^2 - \rho_f^2}{2\rho_b} - \left(\frac{1 + \rho_b^2 - \rho_f^2}{2\rho_b} - 1 \right) \cdot \left(\frac{\rho_b^2 - \rho_f^2}{\rho_b} \right)^2 - 1. \quad (6b)$$

Grain size



Grain size



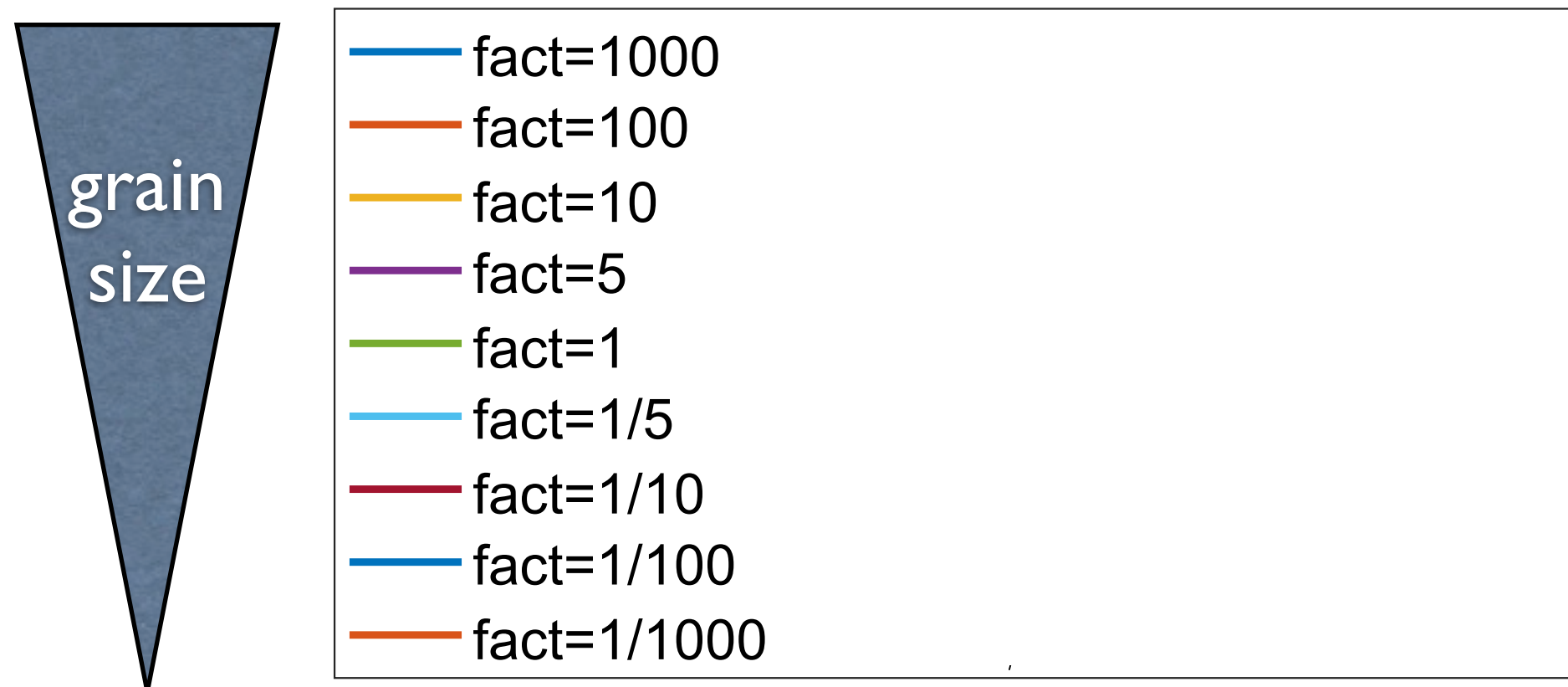
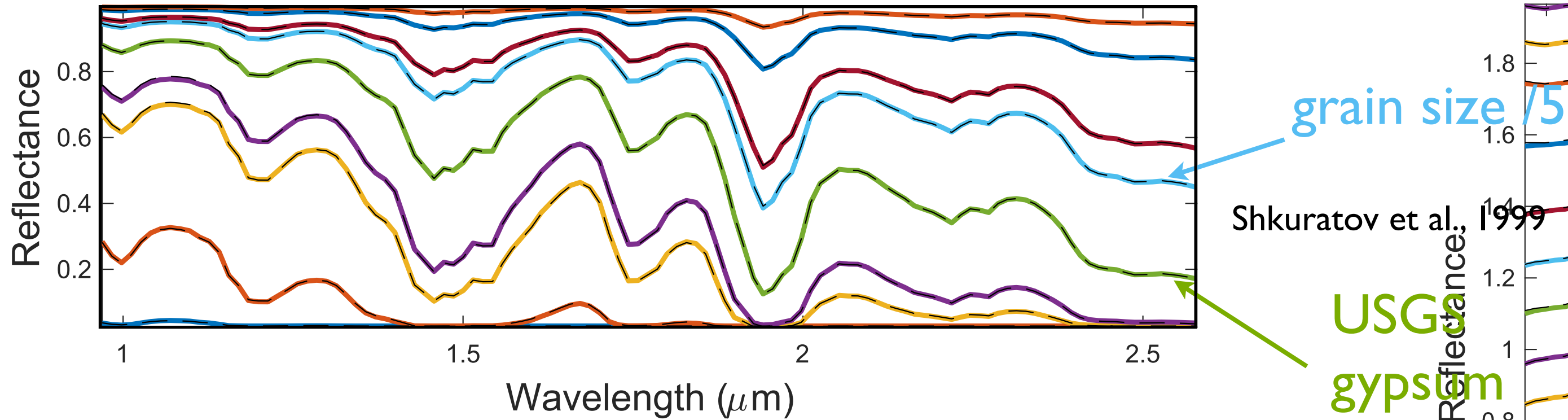
grain size /5

$$I = I_0 \cdot T(\theta_{\text{ext}}) \cdot T(\theta_{\text{int}}) \cdot \exp\left(-\frac{2\tau}{d} \cdot \frac{A}{\cos \theta}\right) \cdot \prod_{v=0}^m R(\theta_v)$$
$$r_b = R_b + \frac{2}{2} \int_0^{\tau} R_b \exp(-2\tau') (1 - R_b \exp(-2\tau'))$$
$$r_t = R_t + \frac{2}{2} \int_0^{\tau} R_t \exp(-2\tau') (1 - R_t \exp(-2\tau'))$$
$$A = \frac{1 + \rho_b^2 - \rho_t^2}{2\rho_b}$$

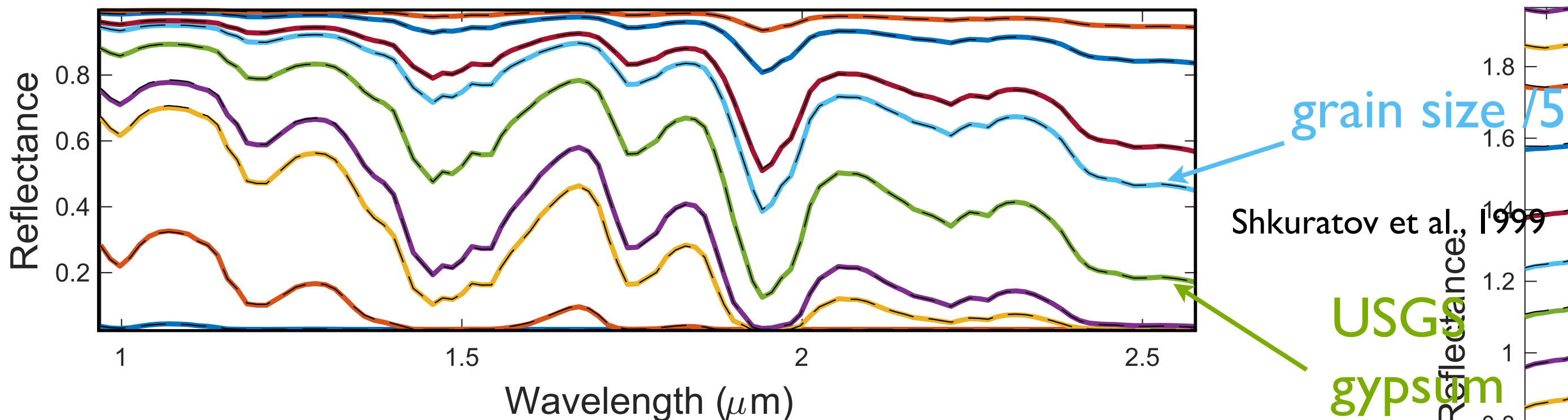
Shkuratov et al., 1999

USGS
gypsum

Grain size



Grain size

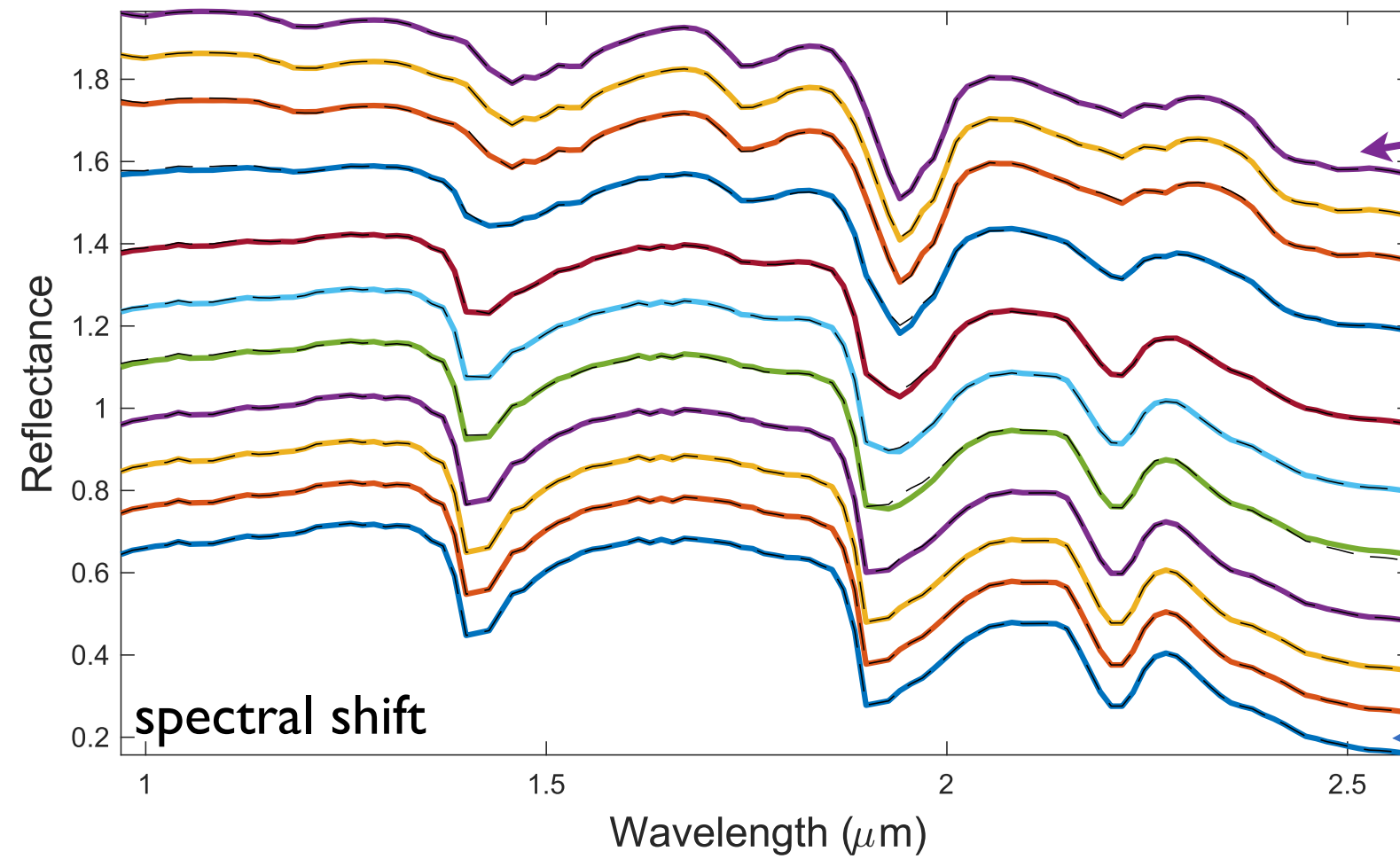


	fact=1000	: $\alpha=36.69$ $\beta=0.03$ RMS=2.5e-04
	fact=100	: $\alpha=10.78$ $\beta=0.03$ RMS=1.9e-03
	fact=10	: $\alpha=3.38$ $\beta=0.02$ RMS=2.4e-03
	fact=5	: $\alpha=2.36$ $\beta=0.02$ RMS=3.0e-03
	fact=1	: $\alpha=1$ $\beta=0$ RMS=0.0e+00
	fact=1/5	: $\alpha=0.45$ $\beta=0$ RMS=1.1e-03
	fact=1/10	: $\alpha=0.32$ $\beta=0$ RMS=1.0e-03
	fact=1/100	: $\alpha=0.1$ $\beta=0$ RMS=4.5e-04
	fact=1/1000	: $\alpha=0.03$ $\beta=0$ RMS=1.5e-04

● excellent fit !

$$Y = \sum_{i=1}^N A_i \cdot S_i^\alpha + \beta$$

Granular mixture



USGS pure gypsum X10

USGS pure smectite /10

$$I = I_0 \cdot T(\theta_{\text{inc}}) \cdot T(\theta_{\text{ref}}) \cdot \exp\left(-\frac{2\mu \cos\theta_{\text{inc}}}{\cos\theta_{\text{ref}}}\right) \cdot \prod_{v=0}^m R(\theta_v)$$

$$r_b = R_b + 2 \frac{\rho_b}{1 + \rho_b} \exp(-2\tau) (1 - R_b \exp(-\tau))$$

$$r_t = R_b \frac{1 - \rho_b \exp(-2\tau)}{1 + \rho_b} \exp(-\tau) + R_b \frac{1 - \rho_b}{1 + \rho_b} \exp(-2\tau)$$

$$A = \frac{1 + \rho_b^2 - \rho_t^2}{2\rho_b}$$

Shkuratov et al., 1999

prop=1:	ab=0.99	$\alpha_1=3.22$	$\alpha_2=230.25$	$\beta=0.01$	RMS=8.6e-05
prop=0.999:	ab=0.99	$\alpha_1=3.22$	$\alpha_2=63.9$	$\beta=0.01$	RMS=8.7e-05
prop=0.99:	ab=0.99	$\alpha_1=3.21$	$\alpha_2=40.27$	$\beta=0.01$	RMS=1.5e-04
prop=0.9:	ab=0.97	$\alpha_1=3.19$	$\alpha_2=26.28$	$\beta=0.03$	RMS=1.3e-03
prop=0.667:	ab=0.95	$\alpha_1=2.25$	$\alpha_2=1.94$	$\beta=-0.03$	RMS=6.9e-03
prop=0.5:	ab=0.75	$\alpha_1=3.1$	$\alpha_2=0.22$	$\beta=0.01$	RMS=2.0e-03
prop=0.333:	ab=0.62	$\alpha_1=3.05$	$\alpha_2=0.24$	$\beta=0.01$	RMS=3.0e-03
prop=0.1:	ab=0.3	$\alpha_1=2.91$	$\alpha_2=0.27$	$\beta=0$	RMS=4.5e-03
prop=0.01:	ab=-0.15	$\alpha_1=0$	$\alpha_2=0.26$	$\beta=-0.01$	RMS=3.3e-03
prop=0.001:	ab=0	$\alpha_1=1.67$	$\alpha_2=0.32$	$\beta=0$	RMS=1.1e-03
prop=0:	ab=-0.08	$\alpha_1=0$	$\alpha_2=0.29$	$\beta=0$	RMS=2.4e-04

● excellent fit !

$$Y = \sum_{i=1}^N A_i \cdot S_i^\alpha + \beta$$

$$Y = \sum_{i=1}^N A_i \cdot S_i^\alpha + \beta$$

- **26 minerals**

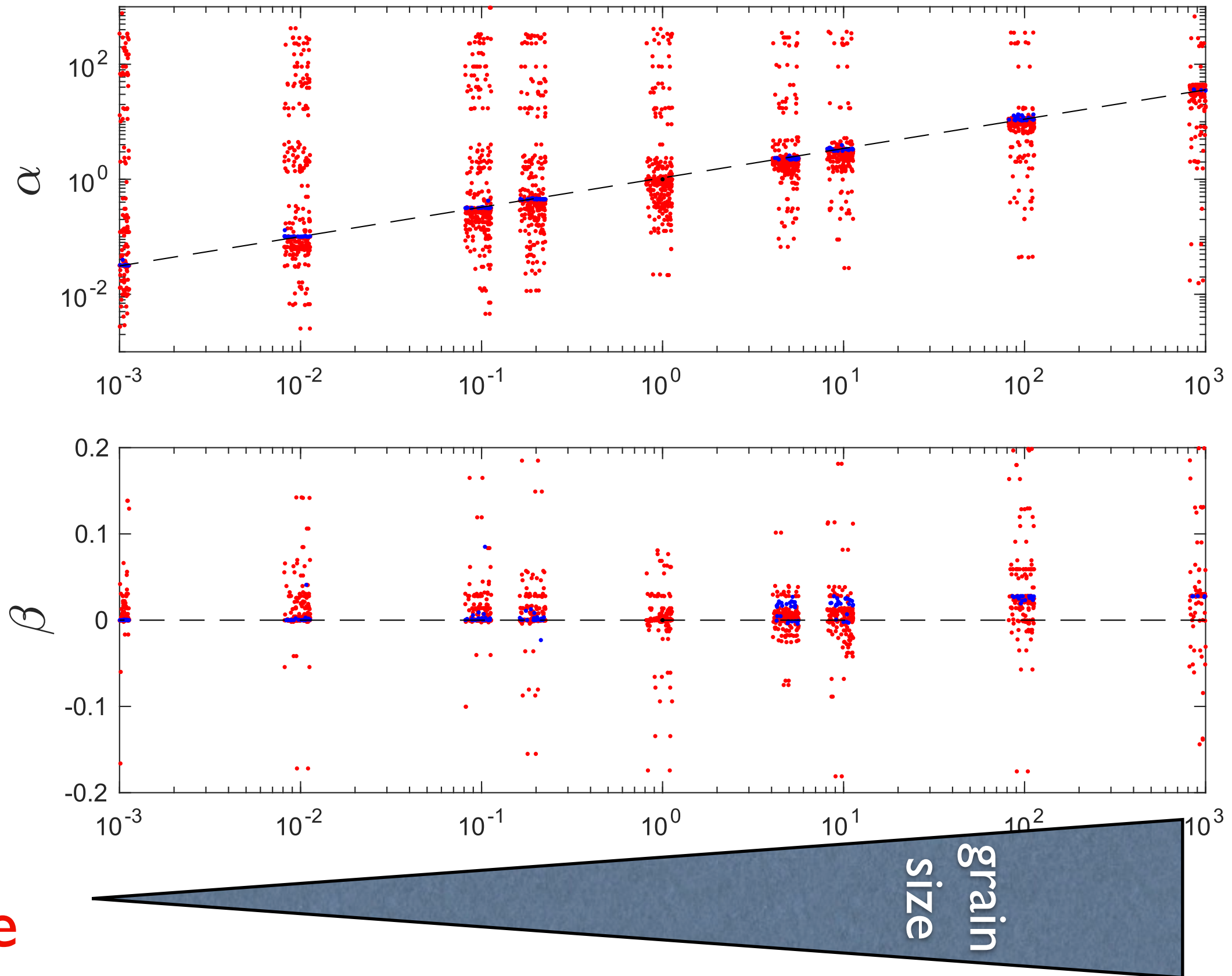
Schmidt, F.; Legendre, M. & Le Mouëlic, S. Minerals detection for hyperspectral images using adapted linear unmixing: *LinMin Icarus*, **2014**, *237*, 61-74, <http://dx.doi.org/10.1016/j.icarus.2014.03.044>

- **Excellent fit**
(98% RMS < 10⁻²)

- **Clear trend for grain size**

- **No trend for granular mixture**

Approximation



Approximation

- Simple **non-linearity** of abundances, under constraints

Schmidt, F. Approximation of Radiative Transfer for Surface Spectral Features *IEEE Geoscience and Remote Sensing Letters*, Institute of Electrical and Electronics Engineers (IEEE), 2023, 20, 1-3, <http://dx.doi.org/10.1109/lgrs.2023.3263356>

$$Y = \sum_{i=1}^N A_i \cdot S_i^\alpha + \beta$$

$$I = I_o \cdot T(\theta_{em}) \cdot T(\theta_{in}) \cdot \exp\left(-\frac{\cos\theta}{\lambda} \sum_{v=0}^m S_v \sin\theta\right) \cdot \prod_{v=0}^m R(\theta_v), \quad (12)$$

$$R_b = \frac{\int_0^{2\pi} d\psi \int_0^{\pi/4} d\theta \cdot R_o(n, \theta)}{\int_0^{2\pi} d\psi \int_0^{\pi/2} d\theta \cdot \cos\theta \cdot \sin\theta} = 2 \int_0^{\pi/4} d\theta \cdot R_o(n, \theta)$$

$$r_b = R_b + \frac{\int_0^{2\pi} d\psi \int_0^{\pi/4} d\theta \cdot R_o(n, \theta) \cdot \exp(-2\tau) / (1 - R_i \exp(-\tau))}{2 \int_0^{2\pi} d\psi \int_0^{\pi/4} d\theta \cdot \cos\theta \cdot \sin\theta}$$

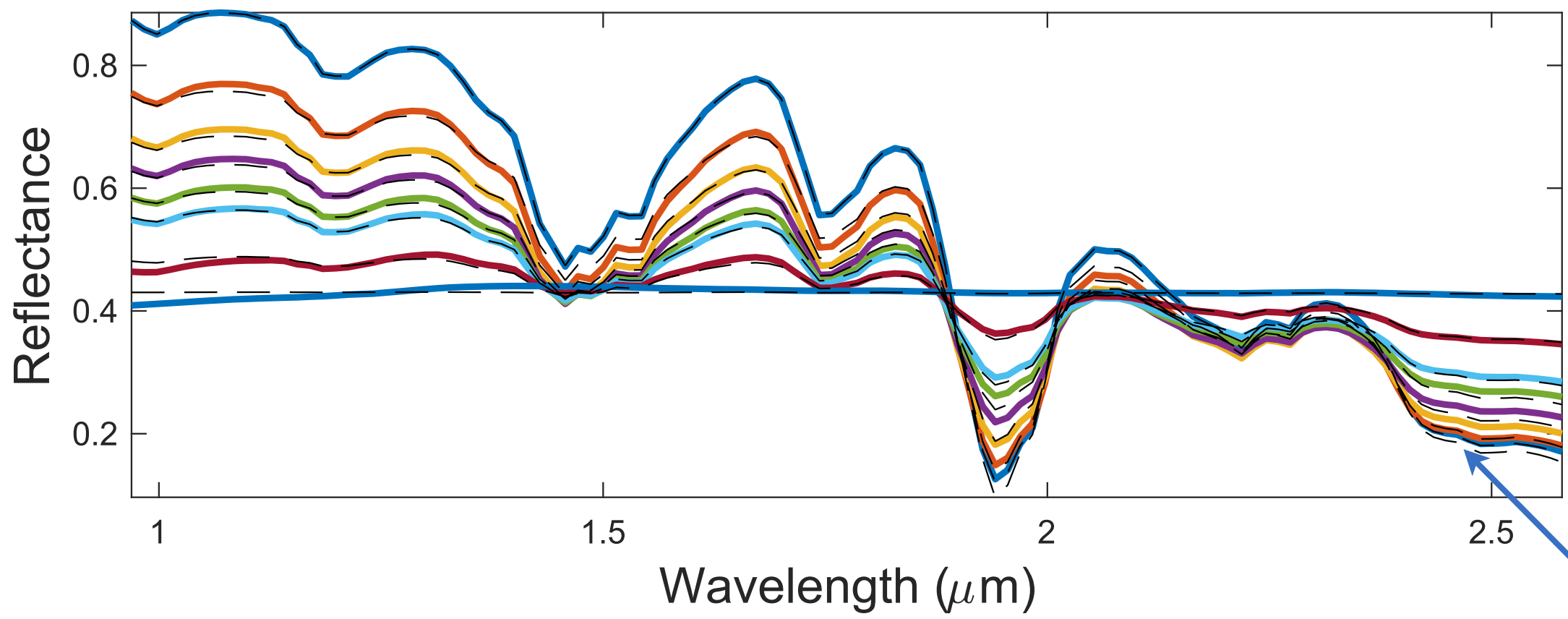
$$A = \frac{1 + \rho_b^2 - \rho_f^2}{2\rho_b} - \frac{\rho_b^2 - \rho_f^2}{2\rho_b} = 1 - \frac{\rho_b^2 - \rho_f^2}{2\rho_b} \quad (6b)$$

- **Test of Martian aerosols effect?**

Aerosols Vincendon et al., 2007;

DISORT Stamnes et al., 1988

Martian aerosols



$$I = I_0 \cdot T(\theta_{\text{sun}}) \cdot T(\theta_{\text{obs}}) \cdot \exp\left(-\sum_{j=1}^m \tau_j \cos^2 \theta_j\right) \cdot \prod_{j=0}^m R(\theta_j)$$

$$r_0 = R_0 + \frac{1}{2} \frac{dR}{d\ln \lambda} \frac{d\ln \lambda}{d\ln \lambda} \exp(-2\tau) \cos^2 \theta$$

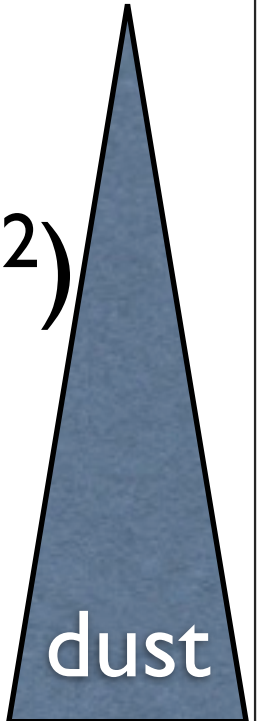
$$r_1 = R_0 + \frac{1}{2} \frac{dR}{d\ln \lambda} \frac{d\ln \lambda}{d\ln \lambda} \exp(-2\tau) \cos^2 \theta + \frac{1}{2} \frac{d^2 R}{d(\ln \lambda)^2} \frac{d(\ln \lambda)^2}{d(\ln \lambda)^2} \exp(-2\tau) \cos^2 \theta$$

$$A = \frac{1 + \beta_0^2 - \beta_1^2}{2\beta_0}$$

Vincendon et al., 2007
Stamnes et al., 1988

USGS pure gypsum

● Excellent fit
(96% RMS < 10⁻²)



—	aot=0.01: $\alpha=0.98$ $\beta=-0.01$ RMS=1.3e-03
—	aot=0.22: $\alpha=0.64$ $\beta=-0.17$ RMS=1.4e-02
—	aot=0.51: $\alpha=0.63$ $\beta=-0.16$ RMS=1.2e-02
—	aot=0.92: $\alpha=0.62$ $\beta=-0.16$ RMS=9.8e-03
—	aot=1.61: $\alpha=0.55$ $\beta=-0.19$ RMS=7.3e-03
—	aot=2.3: $\alpha=0.58$ $\beta=-0.18$ RMS=4.0e-03
—	aot=5: $\alpha=0.26$ $\beta=-0.38$ RMS=5.5e-03
—	aot=20: $\alpha=0.01$ $\beta=-0.56$ RMS=6.7e-03

Approximation

- Simple **non-linearity** of abundances, under constraints

$$\mathbf{Y} = \sum_{i=1}^N A_i \cdot \mathbf{S}_i^\alpha + \beta$$

- **Test of radiative transfer** 
- **Test of Martian aerosols effect** 

NO QUANTIFICATION !

$$\begin{aligned}
 R_b &= \int_0^{2\pi} d\psi \int_0^{\pi/4} d\theta \cdot R_o(n, \theta) \cdot \left(\sum_{v=0}^m S_v \cdot \sin^v \theta \right) \cdot \prod_{v=0}^m R(\theta_v), \\
 &= 2 \int_0^{\pi/4} d\theta \int_0^{2\pi} d\psi \int_0^{\pi/2} d\theta' \cdot R_o(n, \theta) \cdot \left(\sum_{v=0}^m S_v \cdot \sin^v \theta' \right) \cdot \prod_{v=0}^m R(\theta_v), \\
 I &= I_o \cdot T(\theta_{em}) \cdot T(\theta_{in}) \cdot \exp\left(-\frac{2\tau}{\cos \theta} \cdot \sum_{v=0}^m S_v \cdot \sin^v \theta\right) \cdot \prod_{v=0}^m R(\theta_v), \\
 r_b &= R_b + \frac{T_e T_i R_i \exp(-2\tau)}{2 \int_0^{2\pi} d\psi \int_0^{\pi/4} d\theta \cdot R_o(n, \theta) \cdot \cos \theta \cdot \sin \theta} \cdot \left(\sum_{v=0}^m S_v \cdot \sin^v \theta \right) \cdot \prod_{v=0}^m R(\theta_v), \\
 r_f &= R_b + \frac{T_e T_i \exp(-\tau) \cdot \left(\sum_{v=0}^m S_v \cdot \sin^v \theta \right) \cdot \prod_{v=0}^m R(\theta_v)}{2 \int_0^{2\pi} d\psi \int_0^{\pi/4} d\theta \cdot R_o(n, \theta) \cdot \cos \theta \cdot \sin \theta} \cdot \left(\sum_{v=0}^m S_v \cdot \sin^v \theta \right) \cdot \prod_{v=0}^m R(\theta_v), \\
 A &= \frac{1 + \rho_b^2 - \rho_f^2}{2\rho_b} \cdot \left(\frac{2\rho_b}{2\rho_b} \right)^2 - 1. \tag{12}
 \end{aligned}$$

Theory

- Estimation of **endmember spectra (lab)** and **abundances** under constraints:

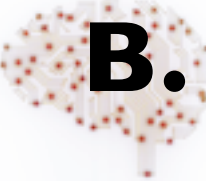
Observation

Number of endmember

$$\mathbf{Y} = \sum_{i=1}^N \mathbf{A}_i \cdot \mathbf{S}_i$$

subject to
positivity
sum-to-one

 A. Non-linearities ? grain size ? aerosols ?

 **B. Large endmember set ?**

Algorithms

dim = 100

$$y(\lambda) = \sum_{i=1}^{N_s} S_i(\lambda) \cdot a_i$$

dim = 50

$$\min \| \mathbf{y} - S\mathbf{a} \|, a_i > 0, \sum_{i=1}^{N_s} a_i = 1$$

- **FCLS**

Heinz, D. & I-Chang, C., TGRS, **2001**, 39, 529-545,

- **MELSUM**

Combe, J.-P.; et al., Analysis of OMEGA/Mars Express data hyperspectral data using a Multiple-Endmember Linear Spectral Unmixing Model (MELSUM): Methodology and first results *Planetary and Space Science*, **2008**, 56, 951-975, <http://dx.doi.org/10.1016/j.pss.2007.12.007>

- **Primal-dual interior-point**

Chouzenoux, E.; Legendre, M.; Moussaoui, S. & Idier, J. Fast Constrained Least Squares Spectral Unmixing Using Primal-Dual Interior-Point Optimization *Selected Topics in Applied Earth Observations and Remote Sensing, IEEE Journal of*, **2014**, 7, 59-69, <http://dx.doi.org/10.1109/JSTARS.2013.2266732>

- **GPU implementation**

Legendre, M.; Capriotti, L.; Schmidt, F.; Moussaoui, S. & Schmidt, A. GPU implementation issues for fast unmixing of hyperspectral images *EGU General Assembly Conference Abstracts*, **2013**, 15, 11686,

- **LIMITATIONS : 50 endmembers << 100 wavelengths**

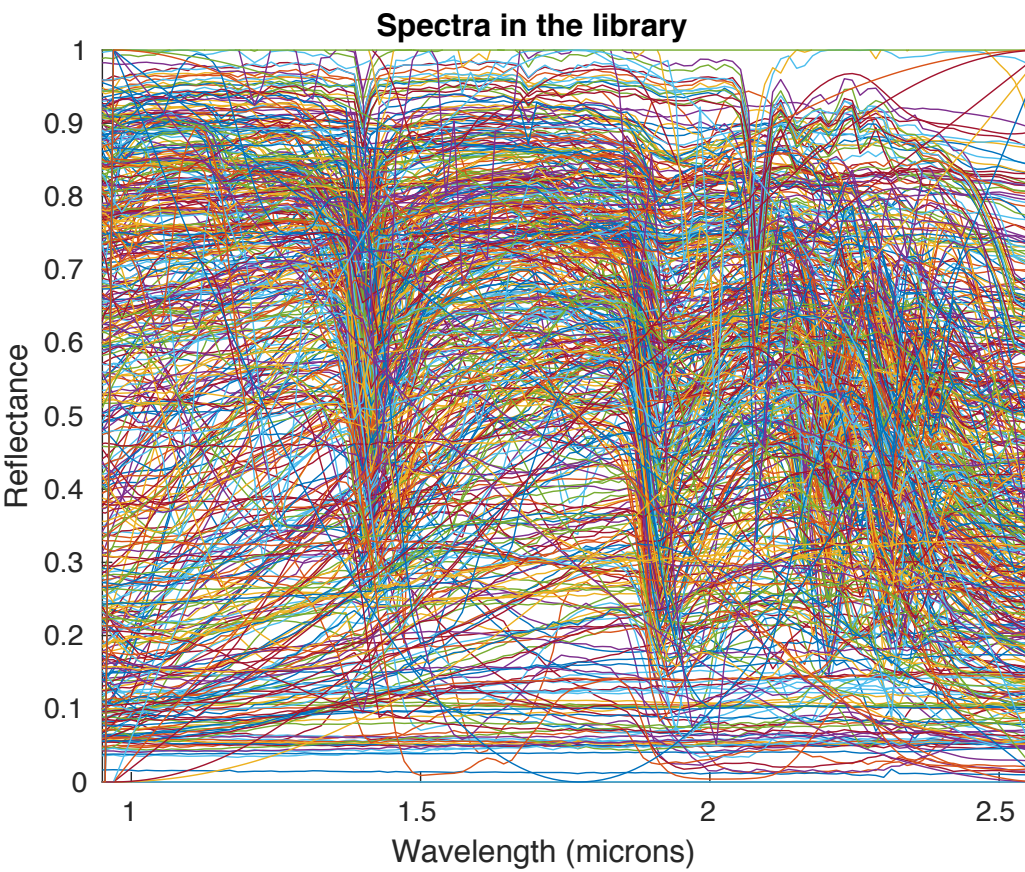
How to deal with large spectral database (500 spectra) ?

Spectral database

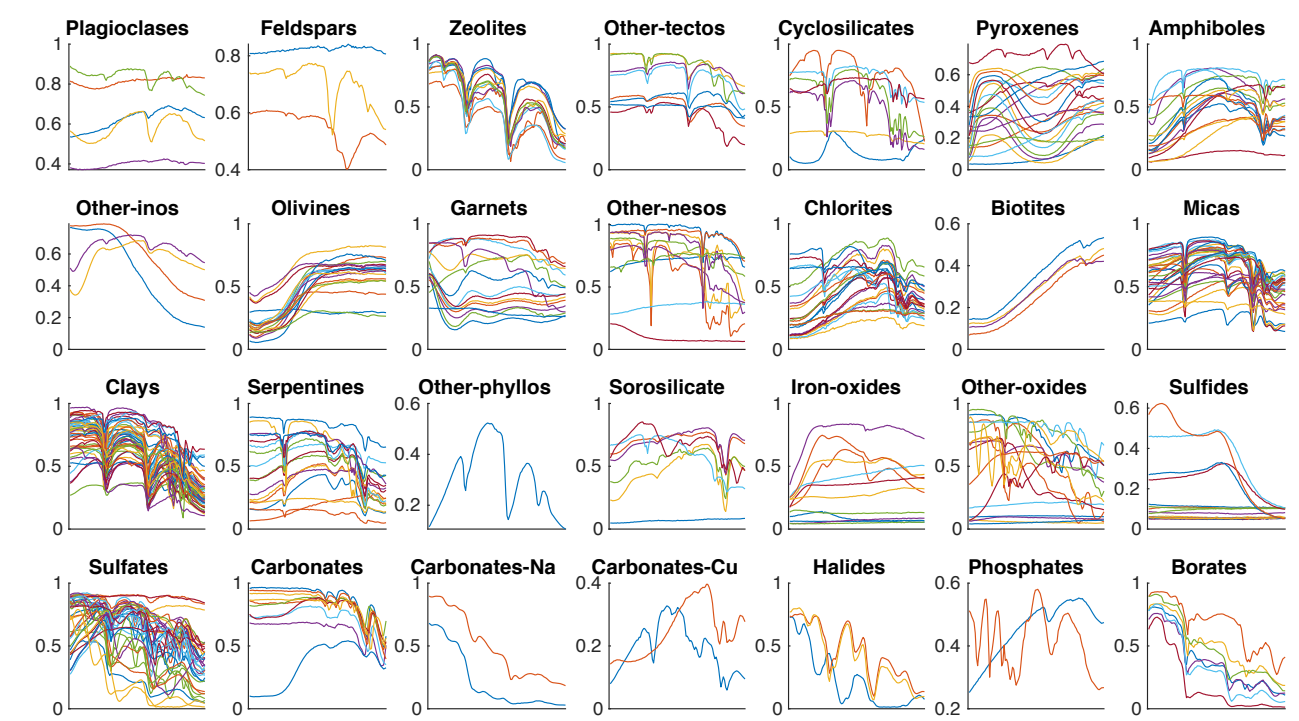
Clark, R. N.; Swayze, G. A.; Wise, R.; Livo, K. E.; Hoefen, T. M.; Kokaly, R. F. & Sutley, S. J. USGS Digital Spectral Library splib05a *U.S. Geological Survey, U.S. Geological Survey, 2003* <http://speclab.cr.usgs.gov/spectral-lib.html>

- Selection of ~500 spectra from USGS

	Family name	Minerals
Tectosilicates	Plagioclases	Andesine Anorthite Bytownite Labradorite Oligoclase
	Feldspars	Adularia Buddingtonite Celsian
	Zeolites	Analcime Chabazite Clinoptilolite Heulandite Laumontite Mordenite Natrolite Scolecite Stilbite Dipyre Lazurite Marialite Mizzonite Nepheline
	Others	
Cyclosilicates		Axinite Beryl Cordierite Elbaite Tourmaline
Inosilicates	Pyroxenes	Acmite Augite Bronzite Diopside Enstatite Fassaite Hedenbergite Hypersthene Jadeite Pigeonite Pyroxene Spodumene
	Amphiboles	Actinolite Amphibole Anthophyllite Cumingtonite Glaucophane Hornblende Hornblende_Fe Hornblende_Mg Richterite Riebeckite Smaragdite Tremolite Uralite
	Others	Pectolite Rhodonite
Nesosilicates	Olivines	Monticellite Olivine Tephroite
	Garnets	Almandine Andradite Grossular Hydrogrossular Spessartine Uvarovite
	Others	Andalusite Datolite Dumortierite Sillimanite Sphene Staurolite Topaz Zircon
Phyllosilicates	Chlorites	Chlorite Clinocllore Clinocllore_Fe Cookeite Corrensite Prochlorite Thuringite
	Biotites	Annite Biotite Siderophyllite
	Micas	Illite Lepidolite Margarite Muscovite Paragonite Phlogopite Rectorite Roscoelite
	Clays	Ammonio-Illite/Smec Ammonio-Smectite Endellite Halloysite Hectorite Kaolinite Montmorillonite Naclite Nontronite Palygorskite Pyrophyllite Saponite Saucanite Sepiolite Talc Vermiculite
	Serpentines	Antigorite Chrysotile Cronstedtite Dickite Lizardite Serpentine
Sorosilicates		Allanite Clinzoisite Epidote Vesuvianite Zoisite
Oxides	Iron oxides	Chromite Ferrihydrite Goethite Hematite Ilmenite Lepidocrocite Maghemite Magnetite
	Others	Brookite Brucite Cassiterite Chalcedony Corundum Cuprite Diaspore Europium_Oxide Gibbsite Manganite Neodymium_Oxide Niter Praseodymium_Oxide Psilomelane Rutile Samarium_Oxide
Sulfides		Arsenopyrite Chalcopyrite Covellite Galena Pyrite Pyrrhotite Sphalerite
Sulfates		Alumite Ammonio-jarosite Ammonioalunite Barite Bassanite Bloedite Butlerite Copiapite Coquimbite Epsomite Eugsterite Gypsum Jarosite Kainite Mascagnite Mirabilite Polyhalite Syngenite
Carbonates		Calcite Dolomite Rhodochrosite Siderite Strontianite Witherite
	Na - rich Cu - rich	Gaylussite Trona Azurite Malachite
Halides		Ammonium Chloride Carnallite
Phosphates		Hydroxyl-Apatite Monazite
Borates		Colemanite Howlite Pinnite Rivadavite Tincalconite Ulexite
Others		Opal



Spectra in the defined families (from 1 to 2.5 microns)



- 27 families of minerals
- 216 groups of minerals

If 3 endmembers, $500 \times 499 \times 498 = 10^8$ combinations to test !!!

Algorithms: Mixed Integer Programming

$$y = Sa \text{ (+ errors)}$$

- $S \rightsquigarrow$ high number of endmembers
 - Spectral variability [Zare and Ho, 2014, Meyer et al., 2016]
- \Rightarrow add more constraints to the problem

Models based on *binary variables* encoding the presence of each member in the data

$$b_n = 1 \Leftrightarrow a_n \neq 0$$

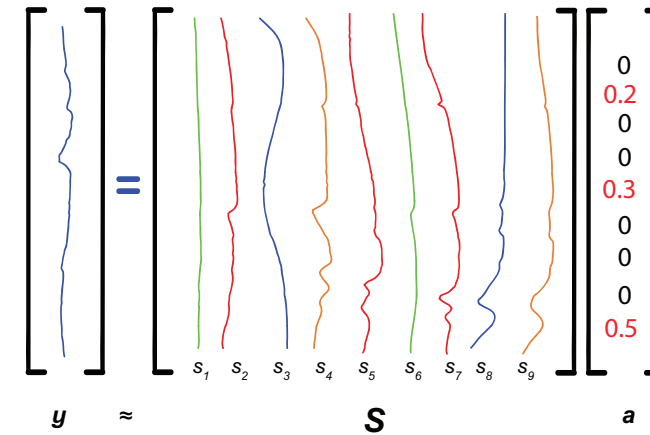
\rightsquigarrow reformulated as $0 \leq a_n \leq b_n$: Mixed Integer Programs

- Sparsity: most abundances are zero [Iordache et al., 2011]
- Structuration of the dictionary into groups [Meyer et al., 2016, Drumetz et al., 2019]
- Minimum values on the nonzero coefficients [never seen ...]

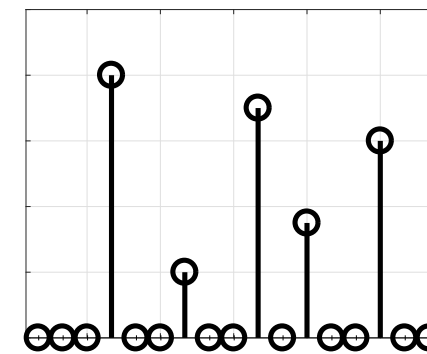
Mixed Integer Programming

Exact ℓ_0 -norm sparsity

- Only a small number of elementary spectra are used for representing the mixture



→ **a** must be sparse:



$$\|\mathbf{a}\|_0 = \text{Card}(n | a_n \neq 0) \leq K$$

- Standard sparse methods perform poorly (ℓ_1 -norm, greedy algorithms)

→ **Exact ℓ_0 -norm constraint:**

$$\min_{\mathbf{a} \in [0,1]^N, \mathbf{b} \in \{0,1\}^N} \frac{1}{2} \|\mathbf{y} - \mathbf{S}\mathbf{a}\|^2 \text{ s.t. } \begin{cases} \mathbf{0} \leq \mathbf{a} \leq \mathbf{b} \\ \sum_{n=1}^N b_n \leq K \\ \sum_{n=1}^N a_n = 1 \end{cases}$$

Constraints in Mixed Integer Programming

- ℓ_0 -norm sparsity

$$\min_{\mathbf{a} \in [0,1]^N, \mathbf{b} \in \{0,1\}^N} \frac{1}{2} \|\mathbf{y} - \mathbf{S}\mathbf{a}\|^2 \text{ s.t. } \begin{cases} \mathbf{0} \leq \mathbf{a} \leq \mathbf{b} \\ \sum_{n=1}^N b_n \leq K \\ \sum_{n=1}^N a_n = 1 \end{cases}$$

- Group Exclusivity **GE**

$$\min_{\mathbf{a} \in [0,1]^N, \mathbf{b} \in \{0,1\}^N} \frac{1}{2} \|\mathbf{y} - \mathbf{S}\mathbf{a}\|^2 \text{ s.t. } \begin{cases} \mathbf{0} \leq \mathbf{a} \leq \mathbf{b} \\ \sum_{i \in G_j} b_n \leq 1 \\ \sum_{n=1}^N a_n = 1 \end{cases}$$

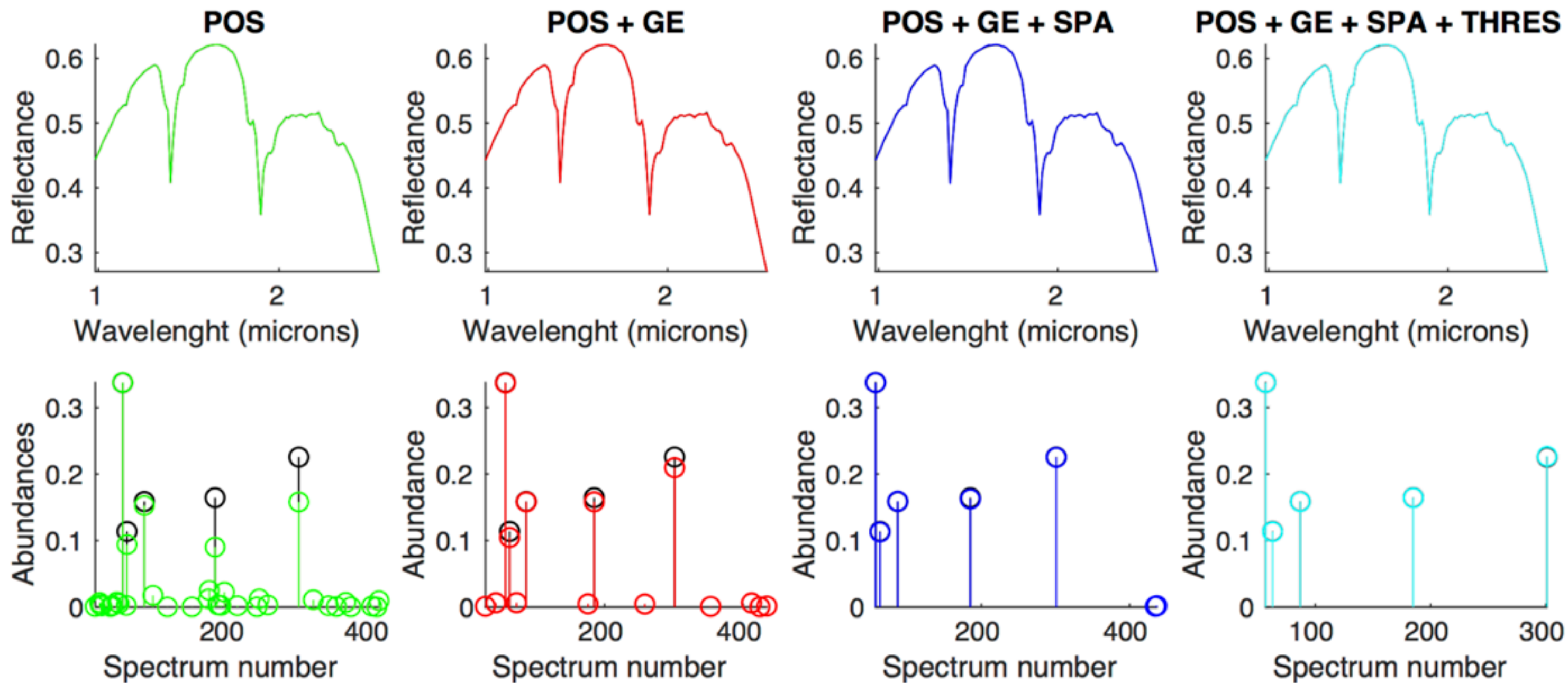
- Significant Abundances **SA**

$$\min_{\mathbf{a} \in [0,1]^N, \mathbf{b} \in \{0,1\}^N} \frac{1}{2} \|\mathbf{y} - \mathbf{S}\mathbf{a}\|^2 \text{ s.t. } \begin{cases} \tau \mathbf{b} \leq \mathbf{a} \leq \mathbf{b} \\ \sum_{n=1}^N a_n = 1 \end{cases}$$

- Efficient resolution *via* numerical MIP solvers (ex. CPLEX)
- These constraints can be mixed

Results

$$y_{\text{simul}} = Sa$$



Results

$$y_{\text{simul}} = Sa$$

$$\min_{x, x_1} \frac{1}{2} \|Y - (Sx + S_1x_1)\|_2^2$$

$$s.t. \|x\|_0 \leq K_{max}$$

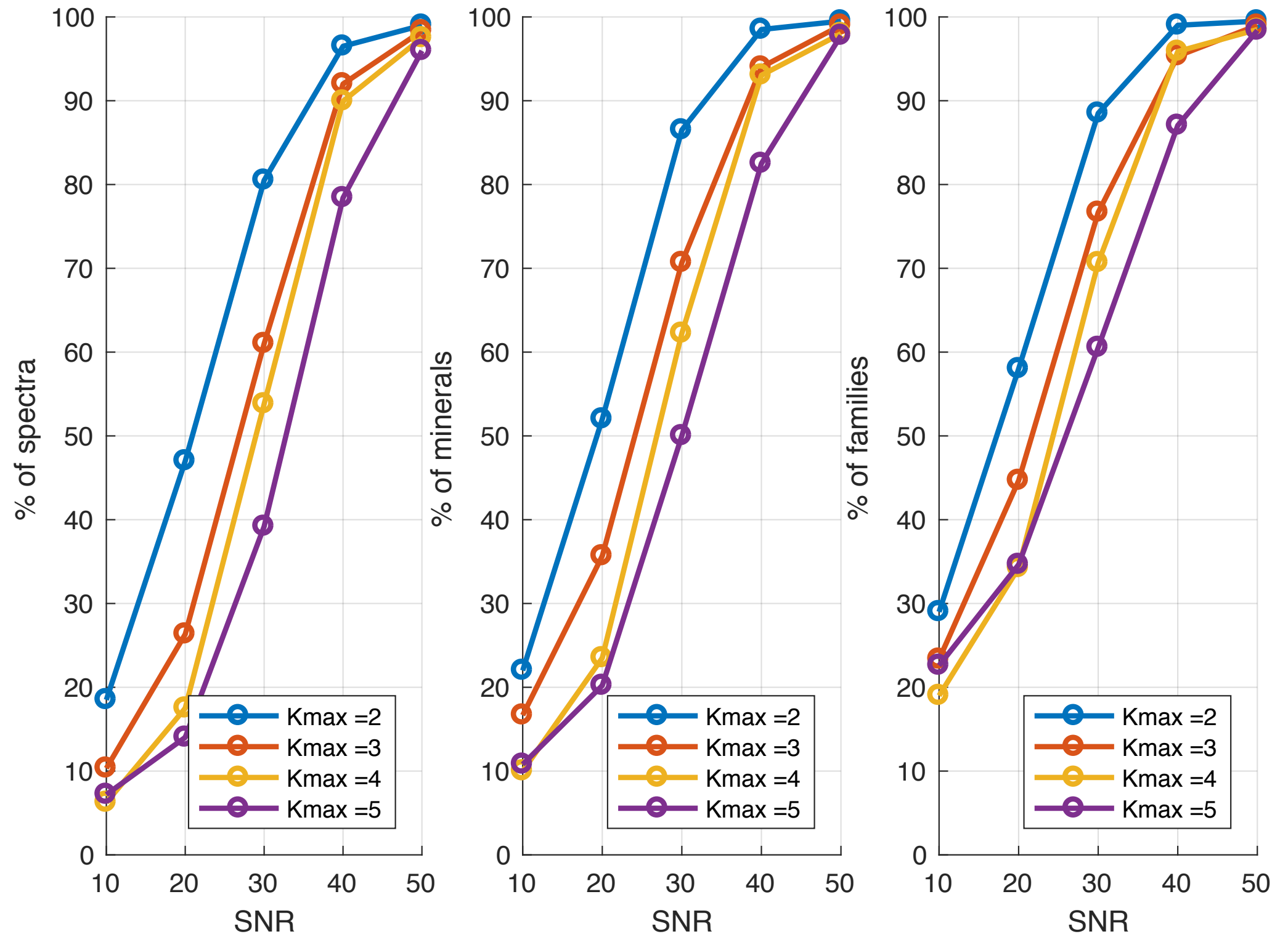
$$s.t. x \geq T$$

$$s.t. \sum x = 1$$

$$s.t. \text{group exclusivity}$$

- Average of 100 runs
- High rate of correct families

Proportion of correct endmembers/minerals/families identified



Results

$$y_{\text{simul}} = Sa$$

0.9

$$\min_{x, x_1} \frac{1}{2} \|Y - (Sx + S_1 x_1)\|_2^2$$

$$s.t. \|x\|_0 \leq K_{max}$$

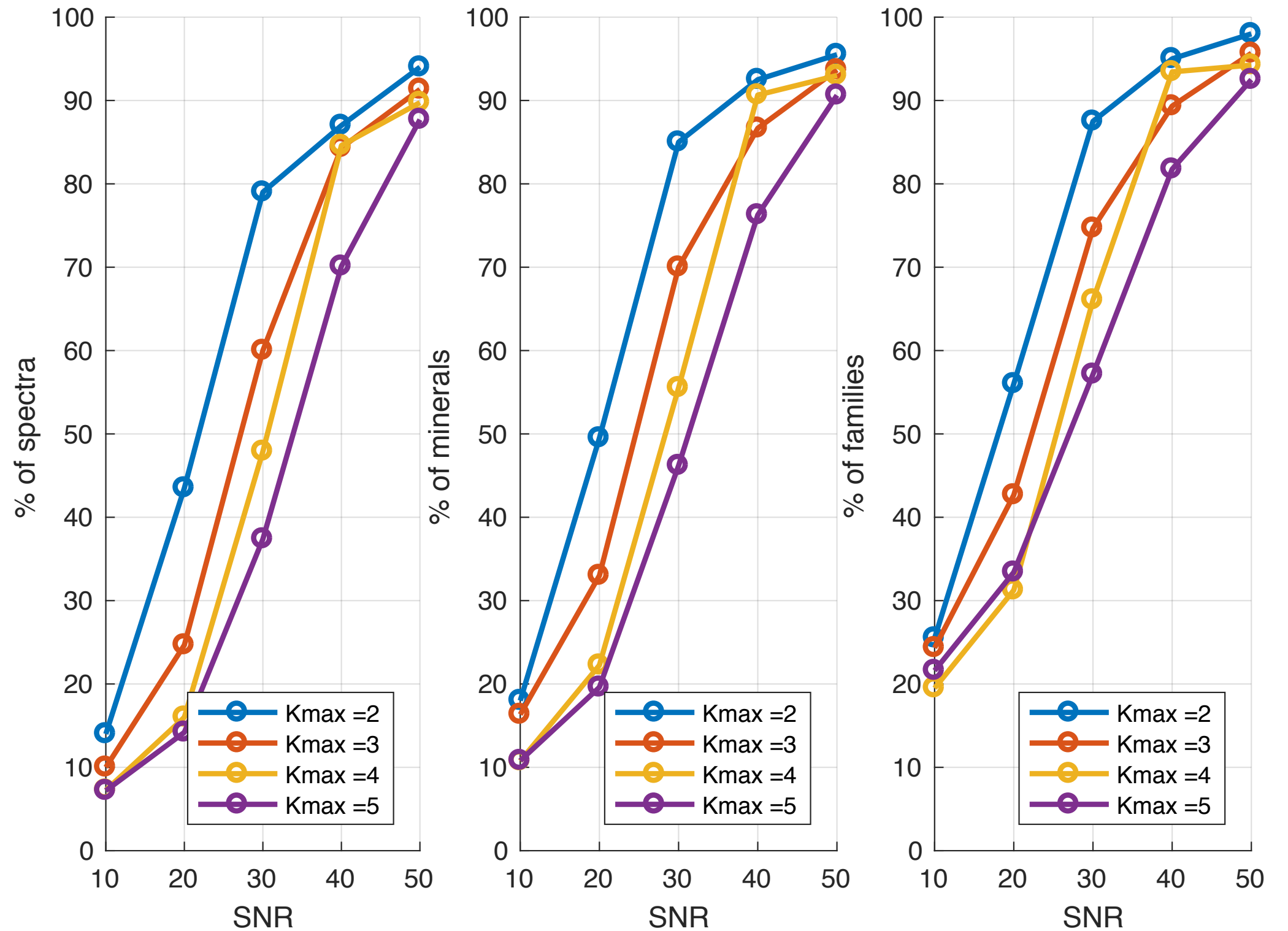
$$s.t. x \geq T$$

$$s.t. \sum x = 1$$

s.t. group exclusivity

- Average of 100 runs
- High rate of correct families

Proportion of correct endmembers/minerals/families identified



Results

$$y_{\text{simul}} = S a^{0.5}$$

$$\min_{x, x_1} \frac{1}{2} \|Y - (Sx + S_1 x_1)\|_2^2$$

$$s.t. \|x\|_0 \leq K_{max}$$

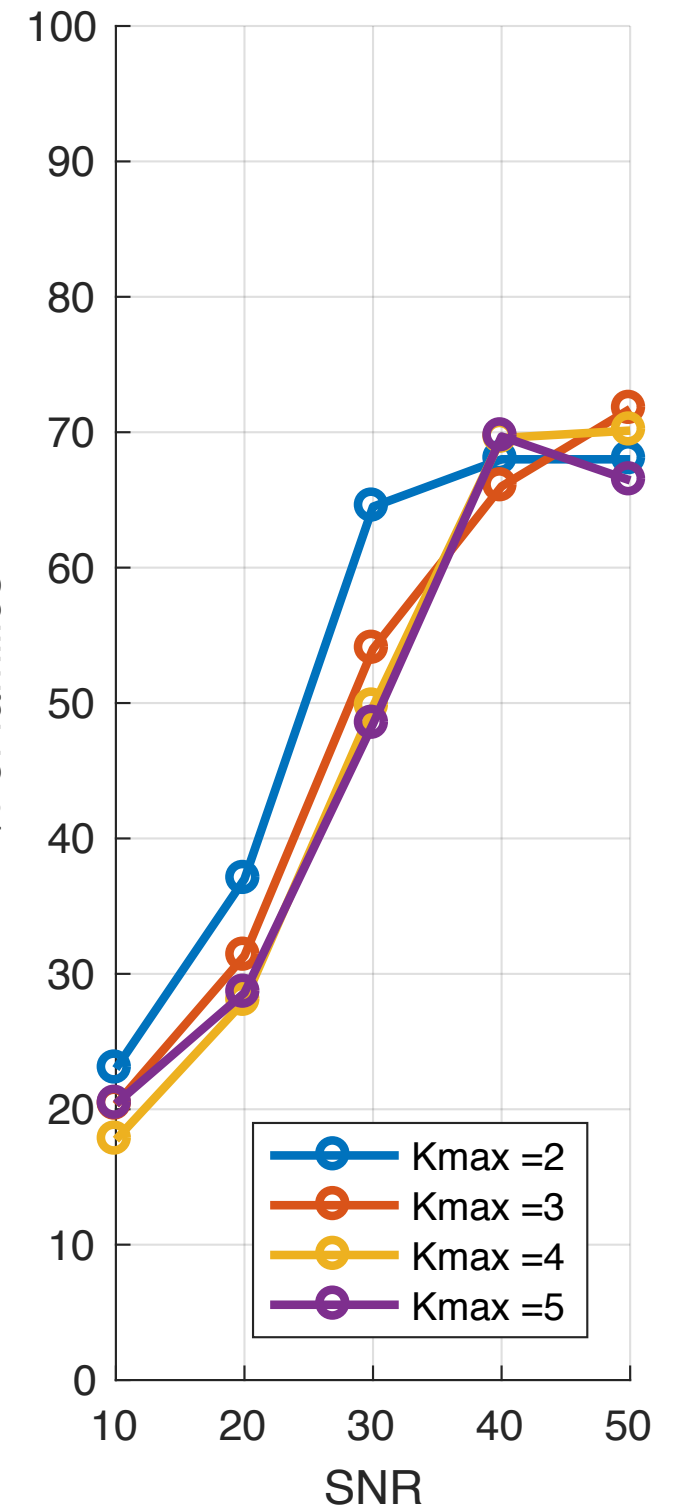
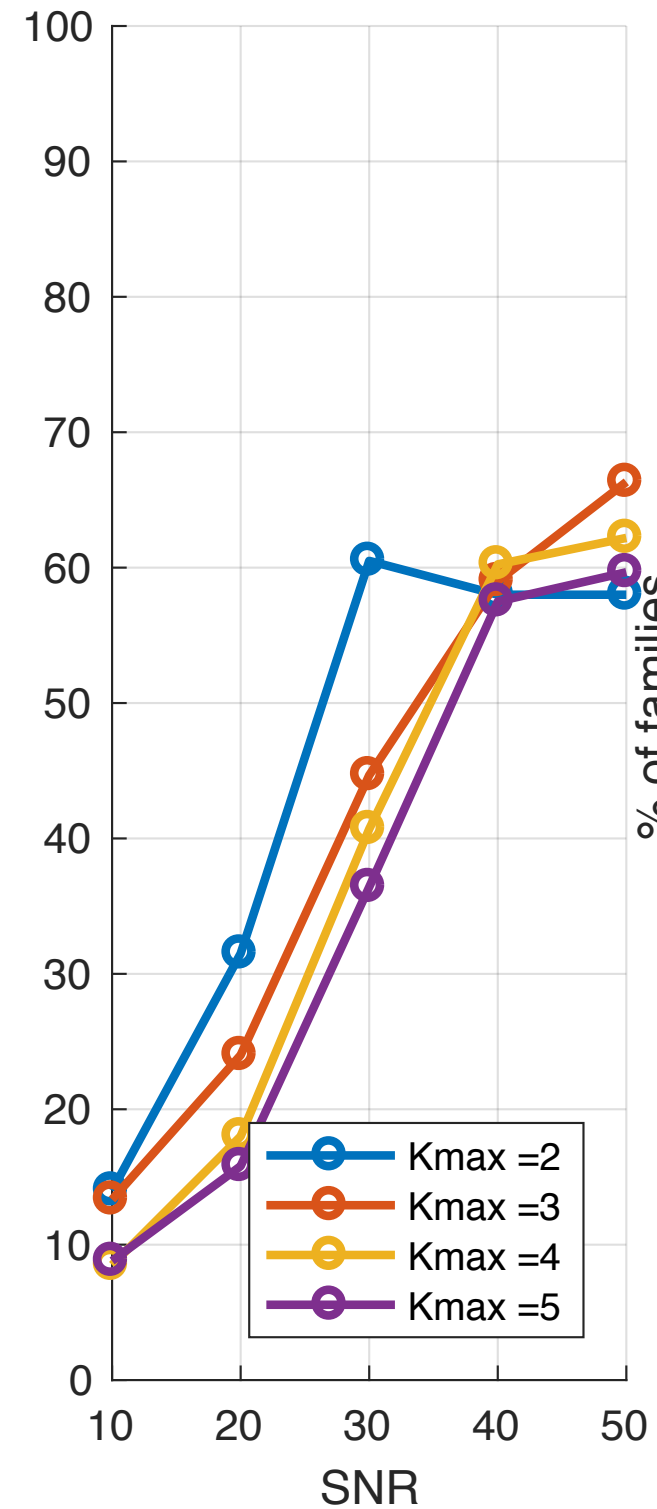
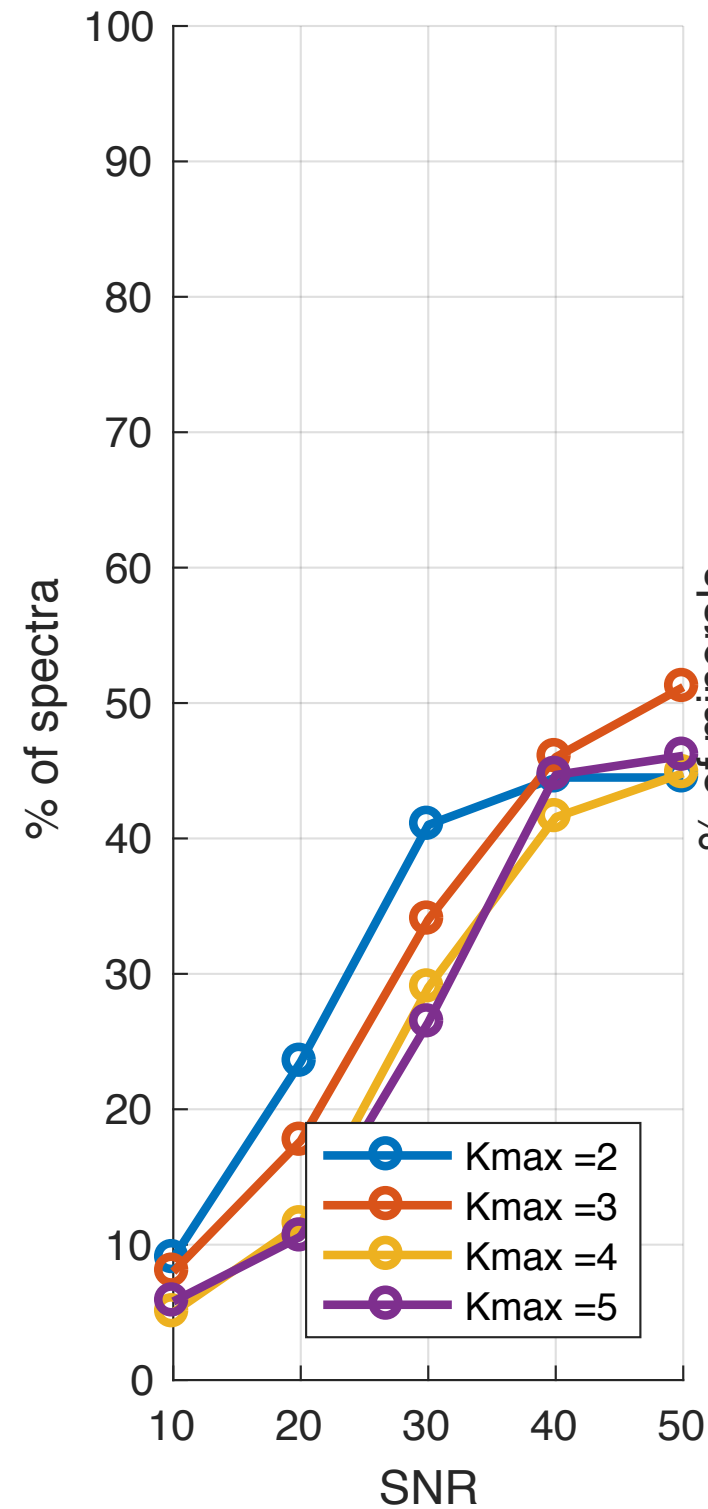
$$s.t. x \geq T$$

$$s.t. \sum x = 1$$

$$s.t. \text{group exclusivity}$$

- Average of 100 runs
- High rate of correct families

Proportion of correct endmembers/minerals/families identified



Conclusion

- New constraints from Mixed Integer Programming (group exclusivity)
- Can handle mineral but also family 
- Family significantly improves the detectability even for ~500 spectra in the database 
- Strong non-linearity still difficult to handle
- Future work : application on real data

Mob Programming

A Whole Team Approach



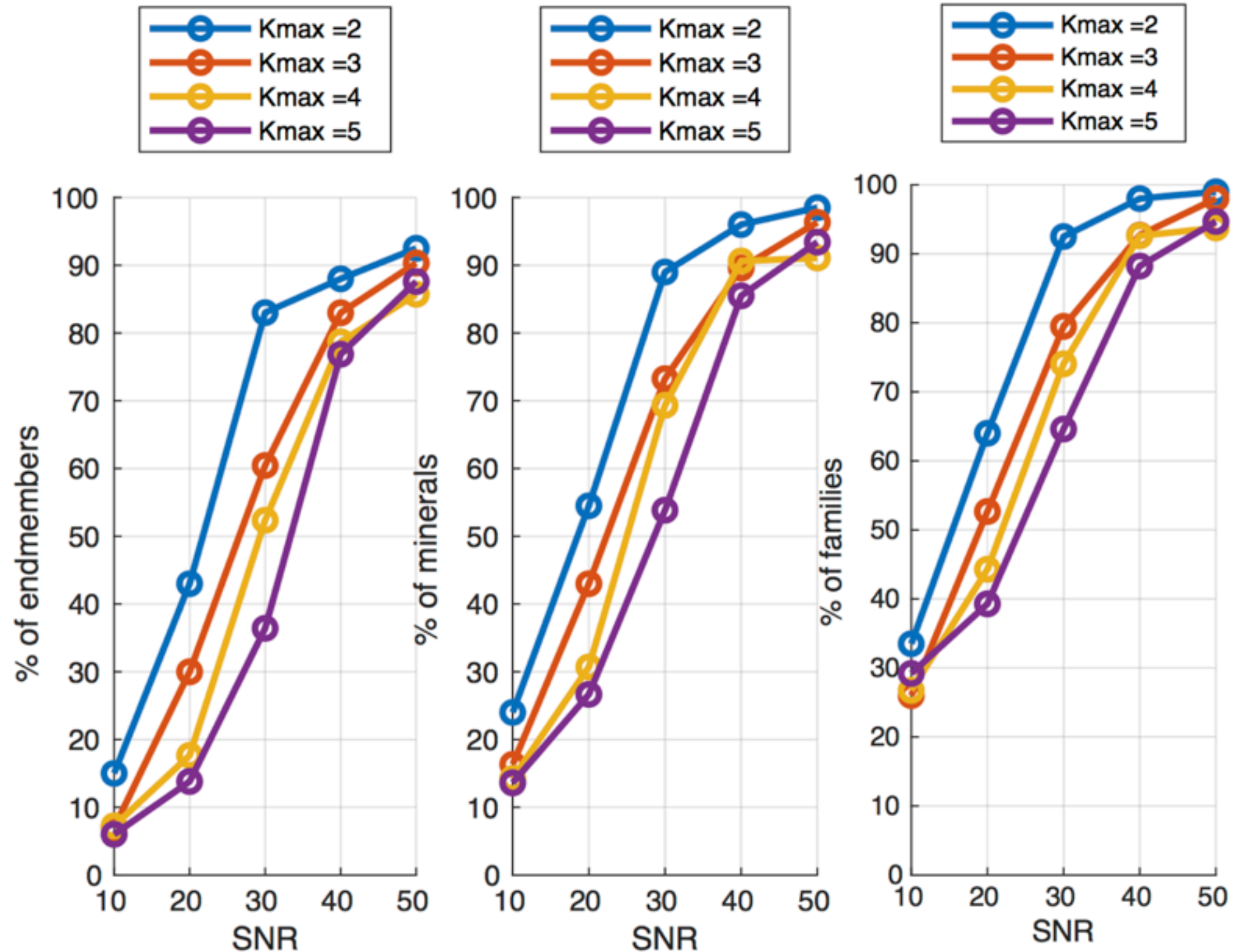
Results

$$y_{\text{simul}} = Sa$$

$$\begin{aligned} \min_x & \frac{1}{2} \|Y - Sx\|_2^2 \\ \text{s.t.} & \|x\|_0 \leq K_{\max} \\ \text{s.t.} & x \geq T \\ \text{s.t.} & \sum x = 1 \\ \text{s.t.} & \text{group exclusivity} \end{aligned}$$

- Average of 100 runs
- High rate of correct families

Proportions of good endmembers/minerals/families identified in the mixture



Results

$$y_{\text{simul}} = Sa + 0.1$$

LEVEL CHANGE

$$\begin{aligned} & \min_x \frac{1}{2} \|Y - Sx\|_2^2 \\ & \text{s.t. } \|x\|_0 \leq K_{\max} \\ & \text{s.t. } x \geq T \\ & \text{s.t. } \sum x = 1 \\ & \text{s.t. } \text{group exclusivity} \end{aligned}$$

- Average of 100 runs
- Middle rate of correct families

Proportions of good endmembers/minerals/families identified in the mixture

